FULL PAPER

Dalton
www.rsc.org/dalton

Synthesis and reactivity of rhodium(I) complexes containing keto-functionalised *N*-pyrrolyl phosphine ligands

Andrew D. Burrows,* Ross W. Harrington, Mary F. Mahon, Mark T. Palmer, Francesco Senia and Maurizio Varrone

Department of Chemistry, University of Bath, Claverton Down, Bath, UK BA2 7AY

Received 3rd June 2003, Accepted 11th August 2003
First published as an Advance Article on the web 28th August 2003

The reaction of $[Rh(\mu\text{-}Cl)(CO)_2]_2$ with two equivalents of L [L = $PR_2\{NC_4H_3C(O)Me\text{-}2\}$; R = Ph, **L^1**; R = NC_4H_4, **L^2**] gave the *P,O*-chelate complexes $[RhCl(CO)(L\text{-}\kappa^2P,O)]$ (**1**, L = **L^1**; **2**, L = **L^2**), whereas reaction with four equivalents of L gave $[RhCl(CO)(L)_2]$ (**3**, L = **L^1**; **4**, L = **L^2**). Complexes **3** and **4** are fluxional in solution, and at low temperatures exist predominantly with one of the two keto groups coordinated. Complexes **3** and **4** undergo metal-promoted hydrolysis reactions with adventitious water leading to the diphosphoxane-bridged dimers $[RhCl(CO)(\mu\text{-}PR_2OPR_2)]_2$ (**5**, R = Ph; **6**, R = NC_4H_4), with the carbonyl and chloride ligands both terminal and semi-bridging in **5** but solely terminal in **6**. Complexes **3** and **4** react with NH_4PF_6 or $TlPF_6$ to give *cis*-$[Rh(L\text{-}\kappa^2P,O)_2]PF_6$ (**7b**, L = **L^1**; **8**, L = **L^2**). These complexes are also formed from the reaction of L with $[Rh(\mu\text{-}Cl)(cod)]_2$ in the presence of NH_4PF_6. Complex **8** reacts with CO to give $[Rh(CO)(\mathbf{L^2})_2]PF_6$ **9**, with PMe_3 to give $[Rh(PMe_3)_2(\mathbf{L^2}\text{-}\kappa^2P,O)]PF_6$ **10**, and with $[NEt_3Bz]Cl$ (Bz = CH_2Ph) to give $[RhCl(\mathbf{L^2}\text{-}\kappa^1P)(\mathbf{L^2}\text{-}\kappa^2P,O)]$ **11**. Complexes **2**, **5**·CH_2Cl_2, **6**·C_7H_8, **7b**, **8** and **11** have been crystallographically characterised. The electron-withdrawing character of **L^1** and **L^2** has led to differences in reactivity from the β-ketophosphine $PPh_2CH_2C(O)Ph$ and the ether-phosphine $PPh_2CH_2CH_2OMe$.

Introduction

Hybrid ligands, carrying a combination of soft and hard donor atoms, continue to attract widespread interest in coordination and organometallic chemistry.[1–4] This attention has concentrated to a large extent on the potential of these ligands to display hemilabile behaviour on platinum group metal centres, and the catalytic opportunities that this reversible generation of vacant coordination sites engenders. The two most important classes of *P,O*-donor ligand that have been studied are ether-phosphines[5–8] and ketophosphines,[9–11] and the chemistry of these two ligand types can differ due to the greater coordinating ability of the carbonyl group, with respect to an ether, towards a late transition metal centre.

We have recently reported the synthesis of the keto-functionalised *N*-pyrrolyl phosphine ligand $PPh_2\{NC_4H_3C(O)Me\text{-}2\}$ **L^1**,[12] and shown that it can act as either a *P*-donor or a *P,O*-donor on molybdenum.[13] The strong π-acceptor character of *N*-pyrrolyl phosphines[14] leads to an enhanced electronic difference between the donor atoms in these ligands, and we reasoned that this could lead to a differentiation in the reactivity of these ligands from other ketophosphines such as $PPh_2CH_2C(O)Ph$. In this paper we report the synthesis of the functionalised tri-(*N*-pyrrolyl)phosphine ligand $P(NC_4H_4)_2\{NC_4H_3C(O)Me\text{-}2\}$ **L^2**, which is anticipated to be a better π-acceptor than **L^1**, and the rhodium(I) chemistry of **L^1** and **L^2**. The use of **L^1** in the rhodium-catalysed hydroformylation of 2-pentene has recently been reported by Beller and co-workers.[15] Some of the results discussed in this paper have been previously reported in a preliminary communication.[16]

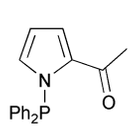

L^1

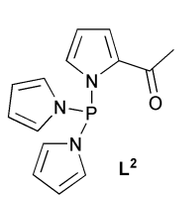

L^2

Results and discussion

Synthesis of $P(NC_4H_4)_2\{NC_4H_3C(O)Me\text{-}2\}$ L^2

The ligand $P(NC_4H_4)_2\{NC_4H_3C(O)Me\text{-}2\}$ **L^2** can be prepared in an analogous manner[12] to **L^1** *via* the reaction of a THF solution of $PCl(NC_4H_4)_2$[15] with 2-acetylpyrrole in the presence of the base NEt_3. The ligand **L^2** was isolated as a colourless crystalline material and characterised by multinuclear NMR and IR spectroscopy. The $^{31}P\{^1H\}$ NMR spectrum of **L^2** showed a singlet at δ 75.1 indicating that the phosphorus is deshielded relative to **L^1**, which was observed at δ 55.8. This is consistent with the pyrrolyl rings acting as stronger electron-withdrawing groups than the phenyl rings, and a similar difference was reported for the *N*-pyrrolyl phosphines $P(NC_4H_4)_3$ (δ 79.6) and $PPh_2(NC_4H_4)$ (δ 48.1).[14]

In the ^1H NMR spectrum of **L^2** the signals for the protons of the 2-acetylpyrrolyl ring appeared as distinctive but unresolved multiplets. The signals for the protons of the non-functionalised pyrrolyl rings appeared as an overlapping doublet of *pseudo* triplets (*pseudo* quintet) at δ 6.74 and a *pseudo* triplet at δ 6.33. The signal for the methyl group was a distinctive singlet at δ 2.35, similar to that observed for **L^1** at δ 2.43.[12] The IR spectrum showed a strong absorption at 1637 cm^{-1} for ν(CO), which is similar to that reported for **L^1** [ν(CO) 1643 cm^{-1}].

Ligand **L^2** is air and moisture sensitive, decomposing both in solution and the solid state to yield intractable purple compounds. Ligand **L^2** reacts rapidly with methanol at ambient temperature with the formation of $(C_4H_4N)_2POMe$ and 2-acetylpyrrole. The functionalised pyrrole ring is selectively substituted, which may simply be a consequence of it being a better leaving group than the unfunctionalised pyrrolyl groups. Alternatively, it is possible that the acetyl functionality plays a role in determining the selectivity, with hydrogen bond formation to the incoming protic nucleophile acting as a directing force in a manner analogous to the mechanism proposed as an explanation for the high reactivity of *N*-pyrazolyl phosphines towards protic reagents.[17]

Synthesis and characterisation of $[RhCl(CO)(L\text{-}\kappa^2P,O)]$ (1, L = L^1; 2, L = L^2)

The reaction of $[Rh(\mu\text{-}Cl)(CO)_2]_2$ with two equivalents of **L^1** or **L^2** in dichloromethane gave the *P,O*-chelate complexes $[RhCl(CO)(\mathbf{L^1}\text{-}\kappa^2P,O)]$ **1** and $[RhCl(CO)(\mathbf{L^2}\text{-}\kappa^2P,O)]$ **2** respectively. Complexes **1** and **2** were characterised on the basis of IR and multinuclear NMR spectroscopy, and the molecular structure of **2** was confirmed by a single crystal X-ray crystallographic study. The IR spectra provided strong evidence for the

DOI: 10.1039/b306292a

coordination of the keto group in the complexes. The ν(C=O) absorption bands were observed at 1576 cm^{-1} for **1** and 1572 cm^{-1} for **2**, both shifted significantly to lower wavenumbers [9,12] with respect to the free ligands. The higher frequency of the metal carbonyl stretch for **2** [ν(CO) 2017 cm^{-1}] compared with **1** [ν(CO) 1989 cm^{-1}] is consistent with $\mathbf{L^2}$ being a better π-acceptor than $\mathbf{L^1}$, as anticipated from the greater number of *N*-pyrrolyl substituents, which reduces the back-donation to the metal carbonyl.

The $^{31}P\{^1H\}$ NMR spectra of **1** and **2** both consisted of a doublet, with that for **1** at δ 93.6 with $^1J_{PRh}$ 178 Hz, and that for **2** at δ 91.4 with $^1J_{PRh}$ 237 Hz. The higher value of $^1J_{PRh}$ in **2** is again indicative of $\mathbf{L^2}$ being a stronger π-acceptor than $\mathbf{L^1}$. In the ^1H NMR spectra of **1** and **2**, the methyl resonances were observed at δ 2.60 for **1** and δ 2.68 for **2**, in both cases shifted downfield with respect to the free ligands which is consistent with coordination of the keto groups.[18] In the $^{13}C\{^1H\}$ NMR spectrum of **2** the signal for the metal carbonyl appeared as a doublet of doublets at δ 183.9 with $^1J_{CRh}$ 78 Hz and $^2J_{CP}$ 19 Hz. The low value of $^2J_{CP}$ indicates a *cis* arrangement of the carbonyl group relative to the phosphorus, which is consistent with the two best π-acceptors avoiding a mutually *trans* arrangement.[19] The signal for the acetyl carbon was observed as a doublet at δ 191.7 with $^2J_{CRh}$ 7 Hz.

These observations can be compared with the analogous reactions of $[Rh(\mu\text{-}Cl)(CO)_2]_2$ with the ether-phosphines $PPh_2(CH_2)_nOMe$ (n = 1,[20] 2, 3[21]) which give the compounds $[RhCl(CO)_2\{PPh_2(CH_2)_nOMe\text{-}\kappa^1P\}]$. This difference in reactivity is consistent with the greater coordinating ability of keto groups with respect to the ether groups in $PPh_2(CH_2)_nOMe$. Whereas $[RhCl(CO)_2(PPh_2CH_2OMe\text{-}\kappa^1P)]$ is stable to CO loss, the compounds $[RhCl(CO)_2\{PPh_2(CH_2)_nOMe\text{-}\kappa^1P\}]$ (n = 2, 3) can be converted to $[RhCl(CO)\{PPh_2(CH_2)_nOMe\text{-}\kappa^2P,O\}]$ by purging solutions with nitrogen, though return to a CO atmosphere leads to the reformation of $[RhCl(CO)_2\{PPh_2(CH_2)_n\text{-}OMe\text{-}\kappa^1P\}]$.[21]

Crystals of **2** suitable for X-ray crystallographic studies were grown by slow diffusion of hexane into a dichloromethane solution. The molecular structure of **2** is shown in Fig. 1, and selected bond distances and angles are given in Table 1. The metal centre has a distorted square-planar coordination geometry with *cis* angles between 86.46(4)° and 91.46(6)°, and a ligand bite angle of 90.66(4)°. As anticipated from the spectroscopic data, the ligand adopts a chelating mode, with the phosphorus atom coordinated *trans* to the chloride. The 6-membered chelate ring assumes a half chair conformation in which the atoms O(1), C(2), C(3), N(1) and P(1) are approximately co-planar, with Rh(1) lying outside this plane. The

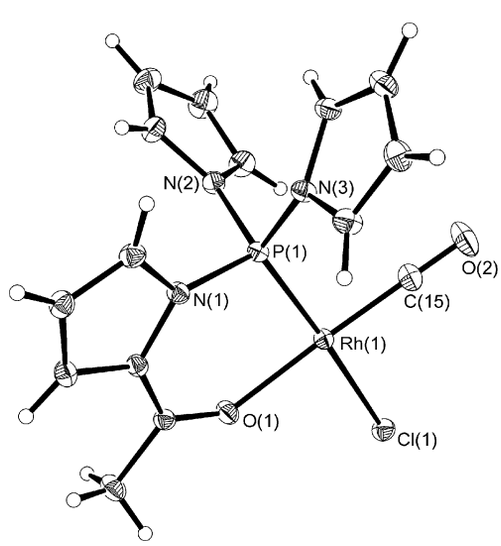

Fig. 1 Molecular structure of $[RhCl(CO)(\mathbf{L^2}\text{-}\kappa^2P,O)]$ **2** with thermal ellipsoids shown at the 30% probability level.

Table 1 Selected bond lengths (Å) and angles (°) for complex **2**

Rh(1)–O(1)	2.0701(12)	P(1)–N(1)	1.7085(14)
Rh(1)–P(1)	2.1474(4)	P(1)–N(2)	1.6965(14)
Rh(1)–Cl(1)	2.3492(4)	P(1)–N(3)	1.6977(15)
Rh(1)–C(15)	1.8152(19)	C(2)–O(1)	1.248(2)
P(1)–Rh(1)–O(1)	90.66(4)	P(1)–Rh(1)–Cl(1)	176.136(16)
O(1)–Rh(1)–Cl(1)	86.46(4)	N(1)–P(1)–Rh(1)	112.66(5)
Cl(1)–Rh(1)–C(15)	91.44(6)	N(2)–P(1)–Rh(1)	115.83(6)
C(15)–Rh(1)–P(1)	91.46(6)	N(3)–P(1)–Rh(1)	121.34(5)
O(1)–Rh(1)–C(15)	177.88(7)		

torsion angle O(1)–C(2)–C(3)–N(1) is 2.9° indicating that the acyl group is essentially co-planar with the pyrrolyl ring.

The Rh(1)–P(1) bond distance is short compared with those reported for the complexes $[RhCl(CO)\{PPh_2(C_6H_4NMe_2\text{-}2)\text{-}\kappa^2P,N\}]$ [2.3308(10) Å[22]] and $[Rh(acac)(CO)\{P(NC_4H_4)_3\}]$ [2.166(1) Å[23]], which is consistent with the electronic character of $\mathbf{L^2}$. The P–N(1) bond distance of 1.7085(14) Å is slightly longer than the P–N(2) and P–N(3) bond distances, though in general the P–N bond distances are similar to those observed in the structure of *trans*-$[RhCl(CO)\{P(NC_4H_4)_3\}_2]$ (av. 1.70 Å).[14] The sum of the angles around each of the nitrogen atoms in **2** are all very close to 360° consistent with their sp^2 hybridisation. The C(2)–O(1) bond distance is longer than that observed in the structure of the ligand $\mathbf{L^1}$ [1.216(2) Å[12]] while being comparable to that in $[MoCp(CO)_2(\mathbf{L^1}\text{-}\kappa^2P,O)][BF_4]$ [1.251(3) Å[13]]. This is indicative of the reduced double bond character of the keto functionalities upon coordination and is in agreement with the IR spectroscopic data.

Synthesis and characterisation of $[RhCl(CO)(\mathbf{L^1})_2]$ 3 and $[RhCl(CO)(\mathbf{L^2})_2]$ 4

The reaction of four equivalents of $\mathbf{L^1}$ with $[Rh(\mu\text{-}Cl)(CO)_2]_2$ in toluene resulted in the evolution of CO and formation of a yellow solution. After 5 minutes stirring, a yellow precipitate of $[RhCl(CO)(\mathbf{L^1})_2]$ **3** began to form, and this was isolated by filtration. A similar reaction of $\mathbf{L^2}$ with $[Rh(\mu\text{-}Cl)(CO)_2]_2$ was carried out in dichloromethane, and in this case the yellow product $[RhCl(CO)(\mathbf{L^2})_2]$ **4** was precipitated by addition of hexane.

The $^{31}P\{^1H\}$ NMR spectra of **3** and **4** both showed broad doublets at room temperature, with that for **3** observed at δ 84.4 with $^1J_{PRh}$ 158 Hz and that for **4** observed at δ 91.4 with $^1J_{PRh}$ 198 Hz. While these parameters are consistent with complexes of the type *trans*-$[RhCl(CO)(L\text{-}\kappa^1P)_2]$, the broadness of the phosphorus resonances reveals the presence of fluxionality on the NMR timescale. The ^1H NMR spectra recorded at ambient temperature also showed broad signals in agreement with the compounds being fluxional. Moreover, since the signal assigned to the protons of the methyl groups in **4** appeared as a broad singlet at δ 2.43 with a chemical shift intermediate between that recorded for complex **2** and for the free ligand $\mathbf{L^2}$, the fluxionality of the complex is likely to involve coordination and dissociation of the keto group. Further support for the presence of such a fluxional process was found in the IR spectra, in which ν(C=O) bands were observed at 1653, 1635 and 1581 cm^{-1}, indicating the presence of both coordinated and uncoordinated acetyl groups.

In order to investigate the fluxional behaviour of complexes **3** and **4** variable temperature NMR spectra were recorded. On cooling a CD_2Cl_2 solution of **3**, the doublet in the $^{31}P\{^1H\}$ NMR spectra progressively broadened, reaching coalescence at approximately −60 °C. At −80 °C a complex group of signals was observed, of which the major component (> 80%) was the AB part of an ABX system (A, B = ^{31}P; X = ^{103}Rh) centred at δ 84.8 with $^2J_{AB}$ 468 Hz, $^1J_{AX}$ 156 Hz and $^1J_{BX}$ 158 Hz. In addition a doublet at δ 83.8 with $^1J_{PRh}$ 149 Hz and two broad singlets at δ 87.1 and δ 82.6 were observed. The major component can be assigned to either the 4-coordinate complex

trans-[Rh(CO)($\mathbf{L^1}$-κ^1*P*)($\mathbf{L^1}$-κ^2*P,O*)]Cl or the 5-coordinate complex [RhCl(CO)($\mathbf{L^1}$-κ^1*P*)($\mathbf{L^1}$-κ^2*P,O*)], both of which contain chemically inequivalent (terminal and chelating) $\mathbf{L^1}$ ligands, while the A_2X spin system is consistent with *trans*-[RhCl(CO)($\mathbf{L^1}$-κ^1*P*)$_2$] which contains magnetically equivalent $\mathbf{L^1}$ ligands. The magnitude of $^2J_{PP}$ in the ABX system and $^1J_{PRh}$ in the A_2X and ABX systems implies that the phosphines are mutually *trans* in both complexes.

On cooling a CD_2Cl_2 solution of **4**, the $^{31}P\{^1H\}$ NMR spectra showed similar behaviour to **3** though with coalescence occurring at the higher temperature of −30 °C. The $^{31}P\{^1H\}$ NMR spectrum of complex **4** recorded at −70 °C is shown in Fig. 2. As for **3**, the major component is the AB part of an ABX spin system, centred at δ 89.3 with J_{AB} 726 Hz, J_{AX} 200 Hz and J_{BX} 202 Hz. In addition, doublets are observed at δ 92.4 and δ 85.1 with J_{AX} of 200 and 202 Hz respectively. This indicates the presence of three compounds, of which the predominant species is either *trans*-[Rh(CO)($\mathbf{L^2}$-κ^1*P*)($\mathbf{L^2}$-κ^2*P,O*)]Cl or [RhCl(CO)($\mathbf{L^2}$-κ^1*P*)($\mathbf{L^2}$-κ^2*P,O*)]. As for **3**, the high values of $^1J_{PRh}$ and $^2J_{PP}$ exclude the possibility of compounds containing mutually *cis* phosphines. For neither **3** nor **4** is it possible to categorically distinguish between *trans*-[Rh(CO)($\mathbf{L}$-κ^1*P*)($\mathbf{L}$-κ^2*P,O*)]Cl and [RhCl(CO)($\mathbf{L}$-κ^1*P*)($\mathbf{L}$-κ^2*P,O*)], or indeed a tight ion pair, on the basis of spectroscopy, though the magnitude of the $^1J_{PRh}$ coupling constants favours a 4-coordinate complex.

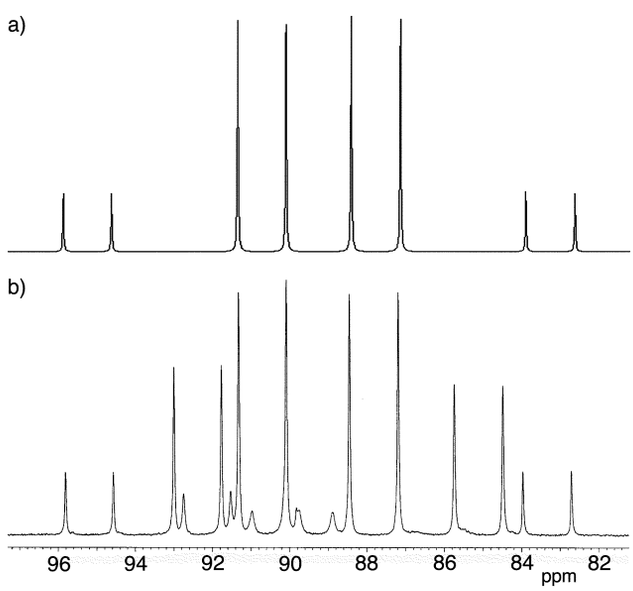

Fig. 2 a) Simulated $^{31}P\{^1H\}$ NMR spectrum for *trans*-[Rh(CO)($\mathbf{L^2}$-κ^1*P*)($\mathbf{L^2}$-κ^2*P,O*)]Cl. b) $^{31}P\{^1H\}$ NMR spectrum of [RhCl(CO)($\mathbf{L^2}$)$_2$] **4** recorded at −70 °C.

The high temperature NMR spectra of **4**, recorded using d^8-toluene as solvent, showed that as the temperature rises the original broad doublet in the $^{31}P\{^1H\}$ NMR spectrum becomes progressively sharper. The $^{31}P\{^1H\}$ NMR spectrum at 50 °C showed a sharp doublet at δ 89.9 with a coupling constant of 209 Hz. This implies that the increase in rate of the fluxional process makes the two phosphorus atoms in **4** chemically equivalent. However, it was found that complex **4** is not thermally stable as evidenced by the appearance of new signals in the $^{31}P\{^1H\}$ NMR spectrum recorded at 60 °C and by an irreversible change in colour of the solution from yellow to dark brown.

In contrast to the observations on **3** and **4**, the β-ketophosphine complex *trans*-[RhCl(CO){$PPh_2CH_2C(O)Ph$-κ^1*P*}$_2$] is not reported to be fluxional,[24] though it can be converted to *trans*-[Rh(CO){$PPh_2CH_2C(O)Ph$-κ^1*P*}{$PPh_2CH_2C(O)Ph$-κ^2*P,O*}]PF_6 on reaction with $TlPF_6$. The analogous reactions with **3** and **4** do not give [Rh(CO)(L-κ^1*P*)(L-κ^2*P,O*)]PF_6: instead the complexes *cis*-[Rh($\mathbf{L^1}$-κ^2*P,O*)$_2$]PF_6 and *cis*-[Rh($\mathbf{L^2}$-κ^2*P,O*)$_2$]PF_6 are formed in high yield following displacement of CO (*vide infra*).

Table 2 $^2J_{PP}$ coupling constants for complexes of general formulae *trans*-[RhX(CO)LL′] and *trans*-[PdI_2LL′]

L	L′	$^2J_{PP}$/Hz	X	Ref.
trans-[RhX(CO)LL′]				
PMe_2Ph	PEt_3	344	Cl	43
PMe_2Ph	PEt_2Ph	348	Cl	43
PMe_2Ph	$PEtPh_2$	352	Cl	43
PMe_2Ph	PPh_3	362	Cl	43
$\mathbf{L^1}$-κ^1*P*	$\mathbf{L^1}$-κ^2*P,O*	468	$\mathbf{L^1}$-κ^2*P,O*	This work
PPr^i_3	$P(OPr^i)_3$	487	Cl	44
PEt_2Ph	$P(OPh)_3$	538	Cl	43
$\mathbf{L^2}$-κ^1*P*	$\mathbf{L^2}$-κ^2*P,O*	726	$\mathbf{L^2}$-κ^2*P,O*	This work
trans-[PdI_2LL′]				
PMe_3	PEt_3	565	I	45
PBu_3	PMe_2Ph	551	I	45
PBu_3	$P(OPh)_3$	758	I	45
PMe_2Ph	$P(OPh)_3$	829	I	45

The extremely high value (726 Hz) of $^2J_{PP}$ between the inequivalent phosphorus atoms observed in the low temperature $^{31}P\{^1H\}$ NMR spectrum of **4** is unusual but not unprecedented. Indeed it is generally observed that the value of $^2J_{PP}$ in transition metal complexes increases with enhancement of their π-accepting character. Examples are reported in Table 2 for complexes of the general formulae *trans*-[RhX(CO)LL′] and *trans*-[PdI_2LL′]. Since $\mathbf{L^2}$ is a strong π-accepting ligand, the value of $^2J_{PP}$ for two inequivalent $\mathbf{L^2}$ ligands is expected to be high.

Comparison of the coalescent temperatures for complexes **3** (*ca.* −60 °C) and **4** (*ca.* −30 °C) suggests that the keto functionality in **4** is more strongly coordinated to the Rh(I) centre than that in **3**. This is consistent with a reduced electron density at the metal centre in complex **4**, in agreement with $\mathbf{L^2}$ being a better π-acceptor/poorer σ-donor than $\mathbf{L^1}$. In a similar manner, the static nature of the complexes [RhCl(CO){$PPh_2CH_2C(O)$-Ph-κ^1*P*}$_2$][24] is in agreement with $\mathbf{L^1}$ and $\mathbf{L^2}$ being better π-acceptor/poorer σ-donor ligands than $PPh_2CH_2C(O)Ph$.

Synthesis and characterisation of [RhCl(CO)(μ-PPh_2OPPh_2)]$_2$ 5 and [RhCl(CO){μ-$P(NC_4H_4)_2OP(NC_4H_4)_2$}]$_2$ 6

Dissolution of [RhCl(CO)($\mathbf{L^1}$)$_2$] **3** in dichloromethane leads to a darkening of colour and precipitation of red crystals after several hours. These crystals are very poorly soluble, and only a broad signal at δ 34.7 could be observed in the $^{31}P\{^1H\}$ NMR spectrum in CD_2Cl_2 after several hours acquisition. The IR spectrum was rather more helpful, with bands observed in the metal carbonyl region at 1964 cm^{-1} and 1793 cm^{-1} but absent from the ν(C=O) region. Taken together with the absence of methyl peaks in the ^1H NMR spectrum, this suggested that rearrangement of $\mathbf{L^1}$ had occurred, with cleavage of the P–N bond and loss of the acetylpyrrolyl group. The crystals were identified by X-ray crystallography as the diphosphoxane complex [RhCl(CO)(μ-PPh_2OPPh_2)]$_2$·CH_2Cl_2, **5**·CH_2Cl_2. The molecular structure of this compound in shown in Fig. 3, with selected bond lengths and angles given in Table 3.

The coordination geometry around each rhodium centre in **5** is distorted trigonal bipyramidal, with two phosphorus atoms from different bridging diphosphoxane ligands arranged *trans* to each other in the axial positions. The equatorial positions are occupied by one terminal and two semi-bridging ligands, which were identified as carbonyls and chlorides, disordered equally between the two positions. This is supported by the IR spectrum, which shows both terminal and bridging metal carbonyls.

Table 3 Selected bond lengths (Å) and angles (°) for complex **5**·CH_2Cl_2[a]

Rh(1) ··· Rh(1)′	2.8683(9)	Rh(1)–Cl(1)	2.360(5)
Rh(1)–P(1)	2.2917(13)	Rh(1)–Cl(2)	2.464(5)
Rh(1)–P(2)′	2.2986(13)	P(1)–O(3)	1.636(3)
Rh(1)–C(26)	1.827(15)	P(2)–O(3)	1.651(3)
Rh(1)–C(27)	1.83(2)		
P(1)–Rh(1)–P(2)′	177.46(5)	Cl(2)–Rh(1)–C(26)	151.7(4)
C(26)–Rh(1)–P(1)	90.8(4)	Rh(1)–C(26)–O(1)	176.3(13)
C(26)–Rh(1)–P(2)′	89.3(4)	Rh(1)–C(27)–O(2)	165.7(12)
Cl(1)–Rh(1)–C(27)	148.5(4)	P(1)–O(3)–P(2)	125.9(2)

[a] Primed atoms generated by the symmetry operation $-x + 1, -y, -z$.

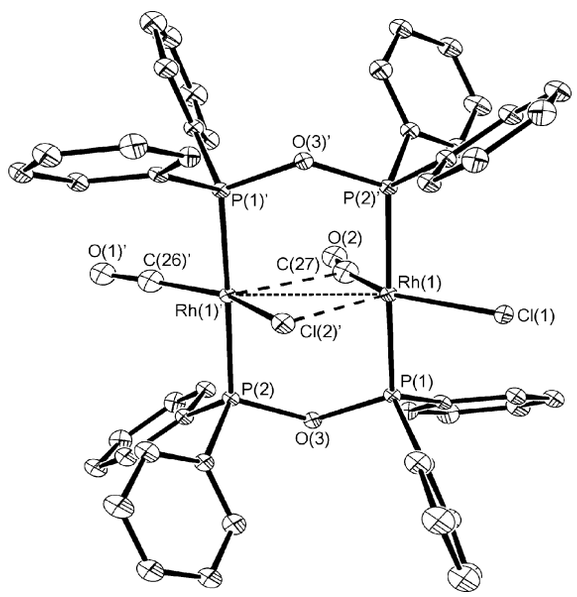

Fig. 3 Molecular structure of $[RhCl(CO)(\mu\text{-}PPh_2OPPh_2)]_2 \cdot CH_2Cl_2$ (**5**·CH_2Cl_2) with hydrogen atoms and the included solvent omitted for clarity and thermal ellipsoids shown at the 30% probability level.

Although a 1 : 1 mixture of the complexes $[Rh_2(CO)_2(\mu\text{-}Cl)_2(\mu\text{-}PPh_2OPPh_2)_2]$ and $[Rh_2Cl_2(\mu\text{-}CO)_2(\mu\text{-}PPh_2OPPh_2)_2]$ cannot be excluded on the basis of the X-ray analysis, a simpler model contains one compound, $[Rh_2Cl(CO)(\mu\text{-}Cl)(\mu\text{-}CO)(\mu\text{-}PPh_2OPPh_2)_2]$, present in two positions with equal likelihood. The related cationic complexes $[Rh_2(CO)_2(\mu\text{-}Cl)(\mu\text{-}CO)(\mu\text{-}L)_2]^+$ (L = dppm, PPh_2NHPPh_2) have previously been structurally characterised.[25–27]

Analysis of the Rh–Rh distances from complexes containing the $Rh_2(\mu\text{-dppm})_2$ skeleton, show that the distance in **5** [2.8683(9) Å] lies within the ranges observed both for compounds which contain a Rh–Rh bond [2.52–3.01 Å, mean 2.77 Å] and for those in which a Rh–Rh bond is absent [2.83–3.47 Å, mean 3.16 Å].[28,29] The P ··· P separation between the phosphorus atoms of the same ligand (2.93 Å) is longer than the Rh–Rh distance indicating compression along the Rh–Rh internuclear axis, though this may be a consequence of the presence of the bridging ligands. These bridges are highly unsymmetrical, with Rh–C(27) distances of 1.83(2) and 2.69(3) Å and Rh–Cl(2) distances of 2.464(5) and 2.889(6) Å respectively, hence the ligands are best described as semi-bridging. This is further reflected in the bond angles, with the bridging carbonyl ligands [Rh(1)–C(27)–O(2) 165.7(12)°] exhibiting a relatively small deviation from the linear conformation observed for the terminal carbonyl [Rh(1)–C(26)–O(1) 176.3(13)°]. Similar semi-bridging carbonyl ligands were observed in the structure of $[Rh_2(\mu\text{-}CO)(CO)_2(\mu\text{-dppm})_2]$.[30] The two diphosphoxane oxygen atoms point in opposite directions in **5** giving a chair conformation for the $Rh_2P_4O_2$ ring, as opposed to the boat conformation observed in the majority of $M_2P_4C_2$ rings.[31]

The oxygen atom in the PPh_2OPPh_2 ligand originates from adventitious water, and this was confirmed by an increase in the rate of formation of **5** from **3** on use of wet dichloromethane. The identity of the solvent is not an important factor in the reaction, and **5** can also be prepared from **3** using wet toluene. Although uncoordinated $\mathbf{L^1}$ is slowly hydrolysed to form $PPh_2P(O)Ph_2$, hydrolysis of **3** to form **5** is much faster under similar conditions, suggesting the reaction is metal-promoted. The chelate complex $[RhCl(PPh_3)(PPh_2OPPh_2)]$ has previously been prepared from a metal-promoted rearrangement and disruption of mutually *cis* $PPh_2O_2CCH{=}CH_2$ ligands.[32] The *trans* orientation of the $\mathbf{L^1}$ ligands in **3** disfavours formation of the analogous monomer $[RhCl(CO)(PPh_2OPPh_2)]$ on hydrolysis, instead promoting formation of the dimer **5** in which the *trans* orientation of the phosphorus donors in maintained.

In order to examine the generality of this reaction, complex **4** was stirred in wet toluene at 60 °C to produce the complex $[RhCl(CO)\{\mu\text{-}P(NC_4H_4)_2OP(NC_4H_4)_2\}]_2$ **6**. Complex **6** was isolated as a red crystalline material and fully characterised. The IR spectrum showed the presence of a terminal carbonyl at 2029 cm^{-1} and the absence of absorption for the acetyl group. On following the reaction by IR spectroscopy, the disappearance of the absorption for **4** is accompanied by the appearance of the absorptions assigned to **6** and 2-acetylpyrrole. The ^1H NMR spectrum showed a *pseudo*-triplet and a *pseudo*-quintet characteristic of the unfunctionalised *N*-pyrrolyl phosphorus substituents, but no signal for the methyl group.

The $^{31}P\{^1H\}$ NMR spectrum of **6** showed a broad apparent doublet of triplets centered at δ 107.3 which is consistent with a dimeric structure. This spectrum is shown in Fig. 4 and can be interpreted as the partially resolved AA′ part of an $[AA'X]_2$ spin system in which X is Rh and A and A′ are the two chemically equivalent but magnetically inequivalent phosphorus atoms of $P(NC_4H_4)_2OP(NC_4H_4)_2$. Although a full analysis of this spectrum is prevented by the observed broadness, it is possible to calculate the values of $^1J_{PRh}$ as 186 Hz and $^3J_{PRh}$ as 3 Hz.

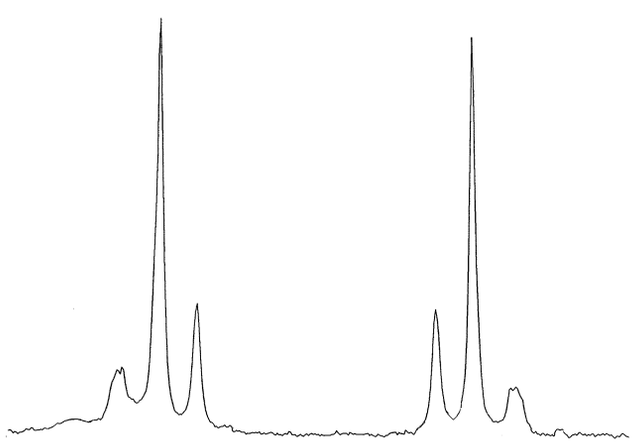

Fig. 4 $^{31}P\{^1H\}$ NMR spectrum of $[RhCl(CO)\{\mu\text{-}P(NC_4H_4)_2OP(NC_4H_4)_2\}]_2$ **6**.

Single crystals of **6**·C_7H_8 were obtained by the slow diffusion of hexane into a toluene solution. The molecular structure of **6** is shown in Fig. 5, and selected bond distances and angles are reported in Table 4. In contrast with **5**, the carbonyl and the chloride in **6** are terminally coordinated and there is no disorder in the dimer. The coordination geometry around each metal centre is distorted square planar with the angles P(1)–Rh–P(2)′ [175.82(2)°] and C(17)–Rh–Cl(1) [170.64(8)°] deviating slightly from the ideal value of 180°. The Rh ··· Rh distance [3.1177(3) Å] is considerably longer than that observed for **5** clearly indicating the absence of a Rh–Rh bond. Although further structural comparisons between **5** and **6** are limited by the disorder

Table 4 Selected bond lengths (Å) and angles (°) for complex **6**·C_7H_8[a]

Rh(1) ··· Rh(1)′	3.1177(3)	P(1)–N(2)	1.6733(18)
Rh(1)–P(1)	2.2664(5)	P(2)–N(3)	1.6948(19)
Rh(1)–P(2)′	2.2624(5)	P(2)–N(4)	1.6716(19)
Rh(1)–C(17)	1.839(3)	P(1)–O(2)	1.6176(15)
Rh(1)–Cl(1)	2.3719(5)	P(2)–O(2)	1.6266(15)
P(1)–N(1)	1.6945(19)		
P(1)–Rh(1)–P(2)′	175.82(2)	P(2)–Rh(1)–Cl(1)′	89.489(19)
C(17)–Rh(1)–Cl(1)	170.64(8)	P(1)–Rh(1)–Cl(1)	91.340(19)
C(17)–Rh(1)–P(1)	89.72(7)	P(1)–O(2)–P(2)	132.42(10)
C(17)–Rh(1)–P(2)′	90.13(7)		

[a] Primed atoms generated by the symmetry operation $-x + 1/2, -y + 1/2, -z$.

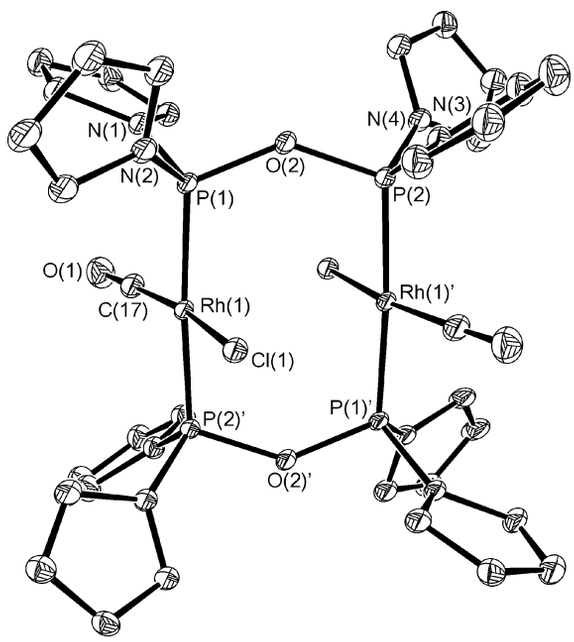

Fig. 5 Molecular structure of [RhCl(CO){μ-P(NC_4H_4)$_2$OP(NC_4H_4)$_2$}]$_2$·C_7H_8 (**6**·C_7H_8) with hydrogen atoms and the included solvent omitted for clarity and thermal ellipsoids shown at the 30% probability level.

in the structure of **5** it is noteworthy that the Rh–P bond distances in **6** [2.2664(5) Å and 2.2624(5) Å] are shorter than those in **5** [2.292(1) Å and 2.299(1) Å], which is consistent with P(NC_4H_4)$_2$OP(NC_4H_4)$_2$ being a better π-acceptor than PPh_2OPPh_2. It is notable that in the formation of **6** the P–N bond to the functionalised pyrrolyl group is selectively cleaved. No evidence was observed for any product in which one of the other P–N bonds had been cleaved.

Synthesis and characterisation of [Rh(L^1-κ^2*P,O*)$_2$]X (7a, X = Cl; 7b, X = PF_6) and [Rh(L^2-κ^2*P,O*)$_2$]PF_6 8

The reaction of four equivalents of **L^1** with [Rh(μ-Cl)(cod)]$_2$ in dichloromethane gave the complex [Rh(**L^1**-κ^2*P,O*)$_2$]Cl **7a**, which was characterised spectroscopically. The $^{31}P\{^1H\}$ NMR spectrum of **7a** consisted of a doublet at δ 108.0 with $^1J_{PRh}$ 204 Hz. The magnitude of this coupling constant suggests that the phosphorus ligands are orientated mutually *cis* such that the phosphorus atoms are both *trans* to the oxygen atoms. The ^1H NMR spectrum showed a deshielding of the methyl protons with δ 2.63, consistent with coordination of the keto groups. This was confirmed by the IR spectrum, which gave a single band for ν(CO) at 1574 cm^{-1}. Complex **7a** was found to decompose readily in solution, precluding a full characterisation. However, the hexafluorophosphate salt, formed on metathesis with NH_4PF_6, is stable in solution, and the complex [Rh(**L^1**-κ^2*P,O*)$_2$]PF_6 **7b** was isolated in the solid state and fully characterised. The NMR and IR spectral parameters for **7b** are similar to those for **7a**, with the addition of signals for the hexafluorophosphate counterion, suggesting that the cations in **7a** and **7b** are identical. The sensitivity of **7a** presumably relates to a competing coordination of the chloride to give [RhCl(**L^1**-κ^1*P*)(**L^1**-κ^2*P,O*)], which is more sensitive than [Rh(**L^1**-κ^2*P,O*)$_2$]$^+$.

The reaction of four equivalents of **L^2** with [Rh(μ-Cl)(cod)]$_2$ in the presence of NH_4PF_6 resulted in the formation of [Rh(**L^2**-κ^2*P,O*)$_2$]PF_6 **8**, which was isolated as a yellow crystalline material following recrystallisation from dichloromethane–hexane. The $^{31}P\{^1H\}$ NMR spectrum of **8** showed a sharp doublet at δ 104.2 with $^1J_{PRh}$ 269 Hz and a septet at δ −143 for the PF_6^- counterion. Whereas the chemical shifts in the $^{31}P\{^1H\}$ NMR spectra of **7** and **8** are very similar, a significant difference exists for the values of $^1J_{PRh}$. As observed before, this is consistent with the electronic difference of the two ligands, with the better π-acceptor ligand giving the higher $^1J_{PRh}$. As with **7b**, coordination of the keto groups can be inferred from the IR spectrum, with ν(CO) observed at 1575 cm^{-1} for **8**.

The NMR spectra for **7b** and **8** are temperature independent, confirming the absence of fluxionality. In the reactions of [Rh(μ-Cl)(cod)]$_2$ with **L^1** and **L^2** there was no evidence for mixed cod–phosphine complexes, in contrast to the reactions of the ether-phosphines $PR_2CH_2CH_2OMe$ (R = Cy, Pr^i, Bu^t and Ph) which give complexes of the general formulae [Rh(cod)(L-κ^2*P,O*)]$^+$ or [Rh(cod)(L-κ^1*P*)$_2$]$^+$.[33]

Complexes **7b** and **8** can also be obtained by chloride abstraction from **3** or **4** with $TlPF_6$ or NH_4PF_6. These reactions proceed with isomerisation to give the thermodynamically more stable product in which the two phosphorus atoms occupy mutually *cis* positions. This is in contrast to the reaction of [RhCl(CO){$PPh_2CH_2C(O)Ph$-κ^1*P*}$_2$] with $TlPF_6$ which gives *trans*-[Rh(CO){$PPh_2CH_2C(O)Ph$-κ^1*P*}{$PPh_2CH_2C(O)Ph$-κ^2*P,O*}]PF_6.[24] The increased lability of the CO ligand in the *N*-pyrrolyl phosphine complexes is a consequence of the stronger π-acceptor character of these ligands which reduces the back-donation to CO.

Single crystals of **7b** and **8** suitable for X-ray analyses were obtained by slow diffusion of hexane into dichloromethane solutions. The structures of the cations of **7b** and **8** are shown in Figs. 6 and 7 respectively, with selected bond distances and angles reported in Table 5. The structures show the two molecules of **L^1** or **L^2** coordinated to the metal centre *via* the phosphorus and oxygen atoms in a distorted square planar geometry with the *cis* arrangement of the ligands consistent with the spectroscopic data. The distortion from square planarity is evident in the *cis* angles which range from 81.57(6)° to 98.748(18)° for **7b**, and from 81.81(7)° to 99.04(2)° for **8**. Crystallographic bite angles of 89.93(4)° and 90.34(4)° for **L^1** in **7b** and 87.71(5)°

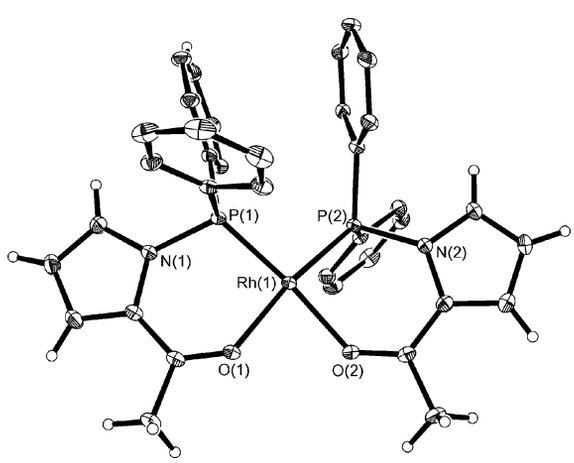

Fig. 6 Molecular structure of [Rh(**L^1**-κ^2*P,O*)$_2$]PF_6 **7b**, with the phenyl hydrogen atoms and the anion omitted for clarity and thermal ellipsoids shown at the 30% probability level.

Table 5 Selected bond lengths (Å) and angles (°) for complexes **7b** and **8**

7b			
Rh(1)–O(1)	2.0880(13)	Rh(1)–P(2)	2.1704(5)
Rh(1)–O(2)	2.0867(14)	P(1)–N(1)	1.7615(16)
Rh(1)–P(1)	2.1680(5)	P(2)–N(2)	1.7525(17)
P(1)–Rh(1)–P(2)	98.748(18)	P(2)–Rh(1)–O(2)	89.93(4)
O(1)–Rh(1)–O(2)	81.57(6)	P(1)–Rh(1)–O(2)	169.36(5)
P(1)–Rh(1)–O(1)	90.34(4)	P(2)–Rh(1)–O(1)	169.80(4)
8			
Rh(1)–O(1)	2.0914(16)	P(1)–N(2)	1.6930(19)
Rh(1)–O(2)	2.0716(16)	P(1)–N(3)	1.690(2)
Rh(1)–P(1)	2.1411(6)	P(2)–N(4)	1.7243(19)
Rh(1)–P(2)	2.1409(6)	P(2)–N(5)	1.692(2)
P(1)–N(1)	1.7297(19)	P(2)–N(6)	1.693(2)
P(1)–Rh(1)–P(2)	99.04(2)	P(2)–Rh(1)–O(2)	91.99(5)
O(1)–Rh(1)–O(2)	81.81(7)	P(1)–Rh(1)–O(2)	167.71(5)
P(1)–Rh(1)–O(1)	87.71(5)	P(2)–Rh(1)–O(1)	171.60(5)

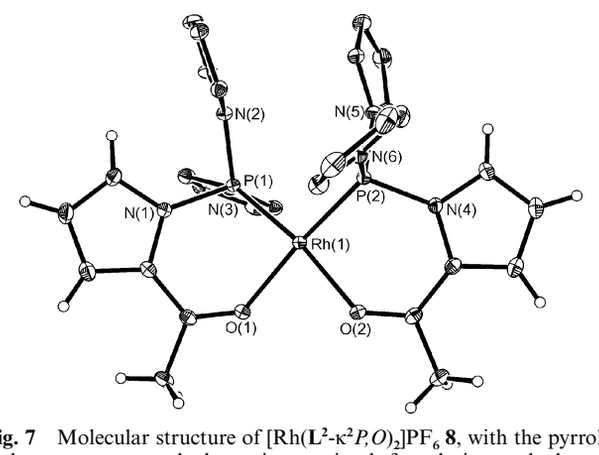

Fig. 7 Molecular structure of $[Rh(\mathbf{L^2}\text{-}\kappa^2\textit{P,O})_2]PF_6$ **8**, with the pyrrolyl hydrogen atoms and the anion omitted for clarity and thermal ellipsoids shown at the 30% probability level.

and 91.99(5)° for $\mathbf{L^2}$ in **8** suggest that the ligands are essentially isosteric, in line with previous observations concerning phenyl and *N*-pyrrolyl groups.[34] The Rh–P distances of 2.1411(6) and 2.1409(6) Å in **8** are significantly shorter than the corresponding distances in **7b** [2.1680(5) Å and 2.1704(5)] indicating the effect of the stronger π-acceptor ligand. The P–N distances in **7b** are longer than those in **8**, and in **8** the P–N bonds to the acetylpyrrolyl group are longer than those to the unfunctionalised pyrrolyl groups.

Reactivity of $[Rh(\mathbf{L^2}\text{-}\kappa^2\textit{P,O})_2]PF_6$

Complexes **7b** and **8** are both stable in dichloromethane, in contrast to *cis*-$[Rh\{PPh_2CH_2C(O)Ph\text{-}\kappa^2\textit{P,O}\}_2]PF_6$ which is slowly oxidised to $[RhCl_2\{PPh_2CH_2C(O)Ph\text{-}\kappa^2\textit{P,O}\}_2]PF_6$.[24] No reaction was observed with either H_2 or methyl iodide, though NMR evidence showed a reaction with CO. When a CD_2Cl_2 solution of **8** was placed under 10 psi CO the $^{31}P\{^1H\}$ NMR spectrum recorded at ambient temperature showed a broad signal at δ 87.2, in addition to the signal for the starting material. Increasing the CO pressure to 20 psi resulted in an increase in intensity of the new signal, though full conversion was not obtained even after prolonged reaction time (24 h). The observed reaction is reversible with release of the CO pressure resulting in complete re-conversion to the starting material. The ^1H NMR spectrum under CO showed in addition to the signals for complex **8** a new set of broad signals. In the aliphatic region a broad singlet at δ 2.30 was clearly distinguishable from the sharp signal for the methyl protons of **8**.

Table 6 $^{31}P\{^1H\}$ NMR spectral parameters for complex **10**. Chemical shifts are in ppm and coupling constants in Hz

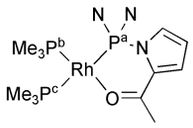

	P^a	P^b	P^c
δ(P)	94.2	8.3	−12.8
$^1J_{PRh}$	273	161	133
$^2J_{PP}$	P^a	P^b	P^c
P^a		49	449
P^b			49

On cooling to −60 °C, the broad signal of the new complex in the $^{31}P\{^1H\}$ NMR spectrum sharpened to give a doublet at δ 84.1 with $^1J_{PRh}$ 188 Hz. The ^1H NMR spectrum at −60 °C showed two sharp singlets in the methyl region at δ 2.73 and δ 2.34, which can be assigned to **8** and the new complex **9** respectively. The chemical shift of the new signal is very similar to that observed for the free ligand $\mathbf{L^2}$, suggesting that in the newly formed complex $\mathbf{L^2}$ is either terminally coordinated through the phosphorus atom or is chelated with the coordination geometry of the metal centre different from that of **8**. Attempts to obtain a low temperature $^{13}C\{^1H\}$ NMR spectrum with a signal to noise ratio high enough to clearly distinguish signals for the carbonyl carbon were unsatisfactory.

Further insight into the identity of **9** was obtained by repeating the variable temperature NMR experiments using ^{13}CO. The $^{31}P\{^1H\}$ NMR spectrum recorded at −75 °C showed a sharp doublet of doublets centred at δ 87.3 with $^1J_{PRh}$ 185 Hz and $^2J_{PC}$ 20 Hz in addition to the signal for the starting material. In the $^{13}C\{^1H\}$ NMR spectrum the coordinated carbonyl group was observed as a doublet of triplets with $^1J_{CRh}$ 74 Hz and $^2J_{CP}$ 20 Hz. The multiplicity of the signals observed in these spectra establish the formula of **9** as $[Rh(CO)(\mathbf{L^2})_2]PF_6$. This is consistent with either the 5-coordinate complex $[Rh(CO)(\mathbf{L^2}\text{-}\kappa^2\textit{P,O})_2]^+$ or the 4-coordinate complex $[Rh(CO)(\mathbf{L^2}\text{-}\kappa^1\textit{P})(\mathbf{L^2}\text{-}\kappa^2\textit{P,O})]^+$ if a fluxional process allowing interconversion of the phosphines is still occurring at this temperature, though in this latter case δ(Me) in the ^1H NMR spectrum would be expected to be similar to that in **4**. Penta-coordinate carbonyl rhodium(I) complexes containing chelating phosphorus ligands have been reported to form from the reaction of $[Rh(dppm\text{-}\kappa^2\textit{P,P})_2]BF_4$ and $[Rh(Ph_2PC_2H_4SPh\text{-}\kappa^2\textit{P,S})_2]BF_4$ with CO.[35,36] However, the reaction of CO with rhodium(I) complexes of ether-functionalised phosphines occurs with displacement of the coordinated oxygen atoms to give tricarbonyl complexes $[Rh(CO)_3(L\text{-}\kappa^1\textit{P})_2]$.[37] Analogous complexes with $\mathbf{L^2}$ can clearly be excluded on the basis of the NMR data.

The addition of one equivalent of PMe_3 to a dichloromethane solution of **8** occurred with displacement of one molecule of $\mathbf{L^2}$ and formation of $[Rh(PMe_3)_2(\mathbf{L^2}\text{-}\kappa^2\textit{P,O})]PF_6$ **10**. Complex **10** was characterised on the basis of its $^{31}P\{^1H\}$ NMR spectrum, which showed three resonances, at δ 94.2 (ddd), δ 8.3 (dt) and δ −12.8 (ddd). Coupling constant information, together with the assignment, is given in Table 6. A similar spectrum has recently been reported for the complex $[Rh(PPh_3)_2\{PPh_2NHC(O)Me\text{-}\kappa^2\textit{P,O}\}]^+$.[38]

It did not prove possible to isolate **10** from a mixture containing **8** and displaced $\mathbf{L^2}$, both of which were also observed in the $^{31}P\{^1H\}$ NMR spectrum.

The reaction of **8** with $[NEt_3Bz]Cl$ produced the complex *cis*-$[RhCl(\mathbf{L^2}\text{-}\kappa^1\textit{P})(\mathbf{L^2}\text{-}\kappa^2\textit{P,O})]$ **11**, which was isolated following recrystallisation from dichloromethane–hexane as red crystals. Complex **11** was fully characterised and its structure was confirmed by X-ray crystallography. The $^{31}P\{^1H\}$ NMR spectrum recorded at ambient temperature showed a broad doublet at δ 98.2 with $^1J_{PRh}$ 276 Hz and the absence of the septet typical of PF_6^-. The high value of $^1J_{PRh}$ is in agreement with a *cis* arrangement of the two phosphorus atoms whereas the appearance of the signal as a broad doublet indicates the presence of a fluxional process which makes the two phosphorus atoms

chemically equivalent. The ^{1}H NMR spectrum showed broad but distinctive signals in the aromatic region and a reasonably sharp singlet at δ 2.49 assigned to the methyl group. The observed chemical shift for the protons of the methyl groups is intermediate between that observed for the coordinated keto groups in **2** (δ 2.68) and for the non-coordinated keto group in the free ligand (δ 2.35) as in **4**, and is consistent with the equilibrium process involving coordination and dissociation of the keto groups. The IR spectrum recorded in dichloromethane showed ν(C=O) for both the uncoordinated and coordinated keto groups at 1642 cm^{-1} and 1592 cm^{-1} respectively, consistent with the NMR data. Similar bands were observed in the solid state IR spectrum, giving a good indication that both coordinated and uncoordinated keto groups were also present in the solid state.

The fluxional behaviour of **11** was studied through variable temperature ^{31}P{^{1}H} and ^{1}H NMR spectroscopy. As the temperature was lowered the original doublet in the ^{31}P{^{1}H} NMR spectrum became progressively broader and reached coalescence at approximately −40 °C. The spectrum recorded at −80 °C showed two doublets of doublets at δ 107.2 and δ 88.0 in agreement with the proposed structure of complex **11**. The broadness of the signals allowed a determination of the values of $^1J_{PRh}$ (275 and 210 Hz) but only an estimate of the value of the *cis*-$^2J_{PP}$ (≈25–30 Hz). The ^{1}H NMR spectrum recorded at −80 °C showed very broad signals in the aromatic region and a relatively sharp signal at δ 2.52 assigned to the methyl groups. The lack of significant broadening of this signal reveals that this temperature is too high to observe coalescence. The etherphosphine complexes [RhCl($PR_2CH_2CH_2OMe$-κ^1*P*)($PR_2CH_2CH_2OMe$-κ^2*P,O*)] (R = Pr^i,[39] Cy[40]) have also been reported to be fluxional, whereas the $PPh_2CH_2C(O)Ph$ analogue is static at room temperature.[24]

The crystal structure of **11** confirmed the formulation proposed on the basis of the spectroscopic data. The unit cell contains two crystallographically independent molecules, though there are only small changes in the interatomic distances and angles for the two independent molecules and therefore only one of these molecules is shown in Fig. 8. Selected bond lengths and angles are given for both molecules in Table 7. The ligands are coordinated to the metal centre in a distorted square planar geometry, with *cis* angles in the range 82.19(14) to 101.22(8)°. The Rh–P bond distances to the monodentate ligands are longer [2.178(2) Å and 2.162(2) Å] than to the ligands forming the chelate rings [2.133(2) Å and 2.135(2) Å]. The latter distances are slightly shorter than the Rh–P distances observed in the structures of [RhCl(CO)(**L**^{2}-κ^2*P,O*)] **2** [2.1474(4) Å] and [Rh(**L**^{2}-κ^2*P,O*)$_2$]PF_6 **8** [av. 2.1410(6) Å]. In both independent molecules, relatively strong intramolecular C–H ··· O hydrogen bonds are observed between a CH group on a pyrrole ring and the uncoordinated keto groups [C(18) ··· O(1) 3.156, H(18) ··· O(1) 2.27 Å, C(18)–H(18) ··· O(1) 156°; C(35) ··· O(4) 3.385, H(35) ··· O(4) 2.46 Å, C(35)–H(35) ··· O(4) 163°].

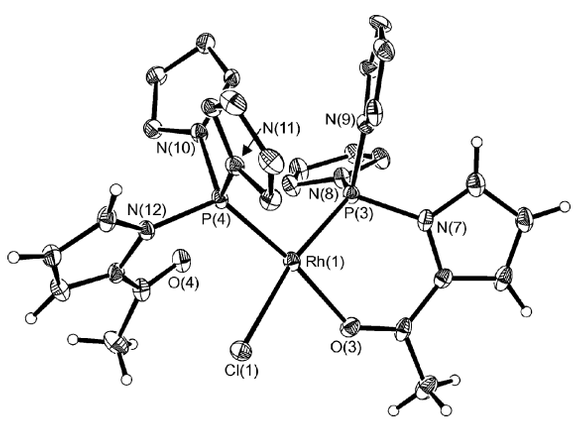

Fig. 8 Molecular structure of one of the independent molecules in the asymmetric unit in [RhCl(**L**^{2}-κ^1*P*)(**L**^{2}-κ^2*P,O*)] **11** with the pyrrolyl hydrogen atoms omitted for clarity and thermal ellipsoids shown at the 30% probability level.

Table 7 Selected bond lengths (Å) and angles (°) for complex **11**

Rh(1)–P(4)	2.178(2)	Rh(2)–P(1)	2.162(2)
Rh(1)–P(3)	2.1332(18)	Rh(2)–P(2)	2.1353(15)
Rh(1)–O(3)	2.093(5)	Rh(2)–O(2)	2.120(6)
Rh(1)–Cl(1)	2.3614(19)	Rh(2)–Cl(2)	2.3416(16)
P(3)–N(7)	1.745(6)	P(1)–N(1)	1.735(5)
P(3)–N(8)	1.705(5)	P(1)–N(2)	1.710(6)
P(3)–N(9)	1.703(7)	P(1)–N(3)	1.710(5)
P(4)–N(10)	1.720(6)	P(2)–N(4)	1.687(6)
P(4)–N(11)	1.709(5)	P(2)–N(5)	1.708(5)
P(4)–N(12)	1.723(5)	P(2)–N(6)	1.721(6)
P(4)–Rh(1)–Cl(1)	92.17(7)	P(1)–Rh(2)–Cl(2)	88.25(7)
Cl(1)–Rh(1)–O(3)	82.19(14)	Cl(2)–Rh(2)–O(2)	84.23(13)
P(3)–Rh(1)–O(3)	88.42(14)	P(2)–Rh(2)–O(2)	86.33(13)
P(3)–Rh(1)–P(4)	97.58(7)	P(1)–Rh(2)–P(2)	101.22(8)
P(3)–Rh(1)–Cl(1)	168.95(7)	P(2)–Rh(2)–Cl(2)	170.52(9)
P(4)–Rh(1)–O(3)	173.11(14)	P(1)–Rh(2)–O(2)	170.25(13)

Conclusions

The synthesis and reactions of rhodium(I) complexes of **L**^{1} and **L**^{2} are summarised in Scheme 1. The strong electron-withdrawing character of the *N*-pyrrolyl phosphine ligands manifests itself in a number of differences between the chemistry of these ligands and the reactions previously reported for etherphosphines such as $PPh_2CH_2CH_2OMe$ and β-ketophosphines such as $PPh_2CH_2C(O)Ph$. Most notably, the rhodium(I) centres in complexes of **L**^{1} and **L**^{2} are relatively electron poor, so the keto groups of **L**^{1} and **L**^{2} tend to be more tightly bound whereas competing π-acceptors such as CO are more weakly bound. Complexes of **L**^{1} and **L**^{2} are less prone to oxidation than those of $PPh_2CH_2C(O)Ph$, again due to the electron-withdrawing character of the ligands.

The differences in the electronic properties of **L**^{1} and **L**^{2} are clearly reflected in both structural and spectroscopic data, with the larger number of electron-withdrawing *N*-pyrrolyl on **L**^{2} leading to this being a poorer σ-donor and better π-acceptor than **L**^{1}. However, in the reactions considered here this electronic disparity does not lead to differences in reactivity.

The P–N bonds in **L**^{1} and **L**^{2} are generally stable to hydrolysis after coordination, but the metal-promoted hydrolysis of the P–N bonds in **3** and **4** has been observed to give the diphosphoxane complexes **5** and **6**. It is noticeable that in the case of **4**, only the bond to the functionalised pyrrole group is cleaved.

Experimental

General experimental

Reactions were routinely carried out using Schlenk-line techniques under pure dry dinitrogen or argon, using dry dioxygen-free solvents unless noted otherwise. Microanalyses (C, H and N) were carried out by Mr Alan Carver (University of Bath Microanalytical Service). Infrared spectra were recorded on a Nicolet 510P spectrometer as KBr pellets, Nujol mulls on KBr discs or in solutions using KBr cells. NMR spectra were recorded on JEOL EX-270, Varian Mercury 400 and Bruker Avance 300 spectrometers referenced to $SiMe_4$ or 85% H_3PO_4. The complexes [Rh(μ-Cl)$(CO)_2]_2$[41] and [Rh(μ-Cl)(cod)]$_2$[42] and the ligand precursor $PCl(NC_4H_4)_2$[15] were prepared following the literature methods. The ligand **L**^{1} was prepared following the previously reported method.[12]

Syntheses

Synthesis of P(NC$_4$H$_4$)$_2${NC$_4$H$_3$C(O)Me-2} L^2. NEt_3 (2.5 cm^3, 18.0 mmol), $PCl(NC_4H_4)_2$ (2.9 g, 14.7 mmol) and 2-acetyl-

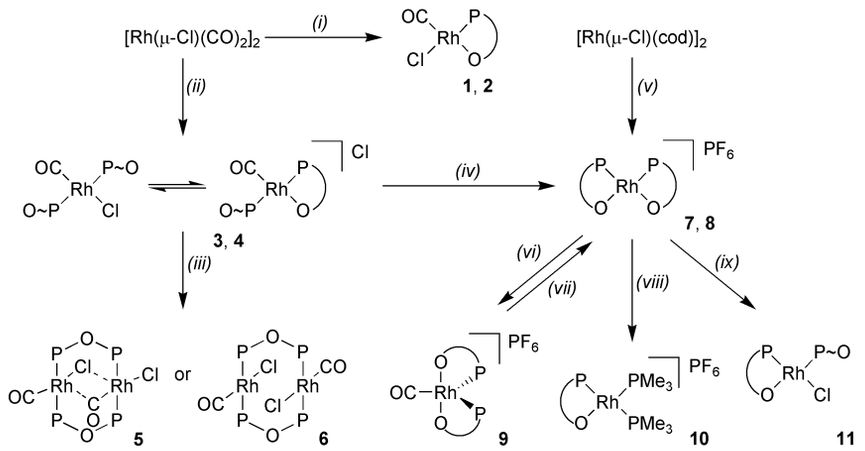

Scheme 1 (*i*) 1 eq. $\mathbf{L^1}$ or $\mathbf{L^2}$; (*ii*) 2 eq. $\mathbf{L^1}$ or $\mathbf{L^2}$; (*iii*) H_2O; (*iv*) $TlPF_6$ or NH_4PF_6; (*v*) 2 eq. $\mathbf{L^1}$ or $\mathbf{L^2}$ + NH_4PF_6; (*vi*) CO; (*vii*) −CO; (*viii*) PMe_3; (*ix*) $[NEt_3Bz]Cl$.

pyrrole (1.60 g, 14.7 mmol) were dissolved in THF (40 cm^3), and the mixture stirred overnight. The colourless precipitate of $[NEt_3H]Cl$ was removed by filtration and washed with THF, and the washings were combined with the filtrate. The volume of this solution was reduced by approximately one half and hexane (30 cm^3) added. Slow evaporation of the solvent produced colourless block shaped crystals which were isolated by filtration and dried under reduced pressure. Yield 3.2 g (80%). $^{31}P\{^1H\}$ NMR (CD_2Cl_2, 161.8 MHz): δ 75.1 (s). ^1H NMR (CD_2Cl_2, 399.8 MHz): δ 7.17 (m, 1H), 6.74 (*ps* quin, 4H), 6.33 (*ps* t, 4H), 6.29 (m, 1H), 5.90 (m, 1H), 2.35 (s, 3H). $^{13}C\{^1H\}$ NMR ($CDCl_3$, 100.5 MHz): δ 188.2 (s), 135.9 (d, $^2J_{CP}$ 2 Hz), 129.8 (d, $^2J_{CP}$ 4 Hz), 122.4 (d, $^2J_{CP}$ 15 Hz), 121.7 (s), 112.8 (s), 112.4 (d, $^3J_{CP}$ 4 Hz), 25.0 (s). IR (KBr, cm^{-1}): 1637s [ν(C=O)].

Synthesis of [RhCl(CO)($\mathbf{L^1}$-κ^2*P,O*)] 1. $[Rh(\mu\text{-}Cl)(CO)_2]_2$ (0.100 g, 0.26 mmol) was added to a stirred solution of $\mathbf{L^1}$ (0.151 g, 0.52 mmol) in dichloromethane (10 cm^3). After 30 min stirring, the solvent was evaporated under reduced pressure. Recrystallisation from dichloromethane–hexane, followed by toluene–dichloromethane–hexane gave orange crystals of **1**. Yield 0.208 g (88%). Calc. for $C_{19}H_{17}ClNO_2PRh$: C, 49.6; H, 3.51; N, 3.05%. Found: C, 49.6; H, 3.60; N, 2.95%. $^{31}P\{^1H\}$ NMR (161.8 MHz, $CDCl_3$): δ 93.6 (d, $^1J_{PRh}$ 178 Hz). ^1H NMR (399.8 MHz, $CDCl_3$): δ 7.65 (m, 1H, C_4H_3), 7.58–7.47 (m, 10H, Ar), 6.96 (br m, 1H, C_4H_3), 6.60 (m, 1H, C_4H_3), 2.60 (s, 3H, Me). IR (KBr, cm^{-1}): 1989vs [ν(CO)], 1576s [ν(C=O)].

Synthesis of [RhCl(CO)($\mathbf{L^2}$-κ^2*P,O*)] 2. $[Rh(\mu\text{-}Cl)(CO)_2]_2$ (0.100 g, 0.26 mmol) was added to a stirred solution of $\mathbf{L^2}$ (0.139 g, 0.51 mmol) in dichloromethane. After 2 h, half of the solvent was evaporated under reduced pressure and hexane was added to precipitate a yellow powder. Recrystallisation from dichloromethane–hexane gave yellow crystals of **2**. Yield 0.216 g (97%). Calc. for $C_{15}H_{14}ClN_3O_2PRh$: C, 41.2; H, 3.22; N, 9.60%. Found: C, 40.8; H, 3.26; N, 9.21%. $^{31}P\{^1H\}$ NMR (161.8 MHz, $CDCl_3$): δ 91.4 (d, $^1J_{PRh}$ 237 Hz). ^1H NMR (399.8 MHz, $CDCl_3$): δ 7.56 (m, 1H), 6.92–6.85 (m, 5H), 6.57 (m, 1H), 6.45 (m, 4H), 2.68 (s, 3H, Me). $^{13}C\{^1H\}$ NMR (100.5 MHz, $CDCl_3$): δ 191.7 (d, $^2J_{CRh}$ 7 Hz), 183.9 (dd, $^1J_{CRh}$ 78 Hz, $^2J_{CP}$ 19 Hz), 133.4 (d, $^2J_{CP}$ 1 Hz), 132.4 (s), 132.0 (d, $^2J_{CP}$ 4 Hz), 123.3 (d, $^2J_{CP}$ 11 Hz), 115.3 (s), 114.8 (d, $^2J_{CP}$ 7 Hz), 27.3 (s, Me). IR (KBr, cm^{-1}): 2017vs [ν(CO)], 1572s [ν(C=O)].

Synthesis of [RhCl(CO)($\mathbf{L^1}$)$_2$] 3. $[Rh(\mu\text{-}Cl)(CO)_2]_2$ (0.050 g, 0.13 mmol) was added to a solution of $\mathbf{L^1}$ (0.151 g, 0.52 mmol) in toluene (10 cm^3) and the mixture stirred for 30 min. The resulting solution was filtered, and the yellow precipitate washed with toluene (5 cm^3) and hexane (20 cm^3) then dried under reduced pressure. Yield 0.178 g (92%). Calc. for $C_{37}H_{32}ClN_2O_3P_2Rh$: C, 59.0; H, 4.28; N, 3.72%. Found: C, 58.7; H, 4.35; N, 3.66%. $^{31}P\{^1H\}$ NMR (161.8 MHz, $CDCl_3$): δ 84.4 (d, $^1J_{PRh}$ 158 Hz). ^1H NMR (399.8 MHz, $CDCl_3$): δ 7.74 (br m, 4H), 7.41 (br m, 6H), 7.14 (dd, 1H, $^3J_{HH}$ 4.0 Hz, $^4J_{HH}$ 1.6 Hz), 6.45 (br m, 1H), 6.21 (t, 1H, $^3J_{HH}$ 4.0 Hz) 2.40 (s, 3H, Me). IR (KBr, cm^{-1}): 1963s [ν(CO)], 1650vs [ν(C=O)]; IR (CH_2Cl_2, cm^{-1}): 1981s [ν(CO)], 1650vs [ν(C=O)].

Synthesis of [RhCl(CO)($\mathbf{L^2}$)$_2$] 4. $[Rh(\mu\text{-}Cl)(CO)_2]_2$ (0.161 g, 0.41 mmol) was added to a solution of $\mathbf{L^2}$ (0.450 g, 1.66 mmol) in dichloromethane. After 2 h stirring hexane was added, resulting in the formation of a yellow precipitate which was isolated by filtration, washed with diethyl ether and dried under reduced pressure. Yield 0.566 g (97%). Calc. for $C_{29}H_{28}ClN_6O_3P_2Rh$: C, 49.1; H, 3.98; N, 11.8%. Found: C, 48.8; H, 3.96; N, 11.4%. $^{31}P\{^1H\}$ NMR (161.8 MHz, CD_2Cl_2): δ 91.4 (br d, $^1J_{PRh}$ 198 Hz). ^1H NMR (399.8 MHz, CD_2Cl_2): δ 7.17 (br, 1H), 7.07 (br, 4H), 6.41 (br, 5H), 5.85 (br, 1H), 2.43 (br, 3H, Me). IR (KBr, cm^{-1}): 1997s [ν(CO)], 1653s, 1635s, 1581w [ν(CO)].

Synthesis of [$Rh_2Cl_2(CO)_2$(μ-PPh_2OPPh_2)$_2$] 5. Complex **3** (0.200 g, 0.27 mmol) was dissolved in dichloromethane (10 cm^3). On standing for 4 h, the initial yellow solution darkened, and red needle-shaped crystals were precipitated. These were separated by filtration, washed with dichloromethane and dried under reduced pressure. Yield 0.101 g (69%). Calc. for $C_{50}H_{40}Cl_2O_4P_4Rh_2{\cdot}CH_2Cl_2$: C, 51.5; H, 3.56%. Found: C, 51.1; H, 3.59%. $^{31}P\{^1H\}$ NMR (CD_2Cl_2, 161.8 MHz): δ 34.7 (br). ^1H NMR (CD_2Cl_2, 399.8 MHz): δ 7.32 (br m). IR (KBr, cm^{-1}): 1964s [ν(CO)], 1793s [ν(CO)].

Synthesis of [$Rh_2Cl_2(CO)_2${μ-$P(NC_4H_4)_2OP(NC_4H_4)_2$}$_2$] 6. Complex **4** (0.200 g, 0.28 mmol) was dissolved in wet toluene (10 cm^3) and stirred at 60 °C for 4 h. A progressive change in the colour from yellow to deep red was observed. On standing at ambient temperature for 48 h, red crystals of complex **6** were deposited. Yield 0.130 g (91%). Calc. for $C_{34}H_{32}Cl_2N_8O_4P_4Rh_2$: C, 40.1; H, 3.17; N, 11.0%. Found: C, 40.3; H, 3.21; N, 11.1%. $^{31}P\{^1H\}$ NMR (161.8 MHz, CD_2Cl_2): δ 107.3 (*ps* dt). ^1H NMR (399.8 MHz, CD_2Cl_2): δ 6.99 (*ps* quin, 16H), 6.34, (*ps* t, 16H). IR (KBr, cm^{-1}): 2029s [ν(CO)].

Synthesis of [Rh($\mathbf{L^1}$-κ^2*P,O*)$_2$]Cl 7a. $\mathbf{L^1}$ (0.119 g, 0.41 mmol) was added to a solution of $[Rh(\mu\text{-}Cl)(cod)]_2$ (0.050 g, 0.10 mmol) in dichloromethane (10 cm^3) and the mixture stirred for 90 min. The solvent was removed under reduced pressure, and the solid washed with cold hexane then dried under reduced pressure. Yield 0.143 g (97%). $^{31}P\{^1H\}$ NMR (161.8 MHz, $CDCl_3$): δ 108.0 (br d, $^1J_{PRh}$ 204 Hz). ^1H NMR (399.8 MHz, $CDCl_3$): δ 7.88 (m, C_4H_3), 7.68–6.88 (br m, Ar), 6.67 (br m, C_4H_3), 6.37 (br m, C_4H_3), 2.63 (s, Me). IR (KBr, cm^{-1}): 1574s [ν(C=O)].

Synthesis of [Rh(L^1-κ^2*P,O*)$_2$]PF$_6$ 7b. NH_4PF_6 (0.034 g, 0.21 mmol) was added to a solution of **7a** formed *in situ* from [Rh(μ-Cl)(cod)]$_2$ (0.050 g, 0.10 mmol) and **L^1** (0.119 g, 0.41 mmol) in THF (30 cm^3). The mixture was stirred for 2 h, then the solution was filtered to remove NH_4Cl. The solvent was removed from the filtrate under reduced pressure, and the crude solid washed with cold diethyl ether and recrystallised from dichloromethane–hexane to give orange crystals of **7b**. Yield 0.154 g (91%). Calc. for $C_{36}H_{32}F_6N_2O_2P_3Rh{\cdot}0.25CH_2Cl_2$: C, 50.9; H, 3.83; N, 3.27%. Found: C, 50.9; H, 3.93; N, 3.16%. $^{31}P\{^1H\}$ NMR (161.8 MHz, CD_2Cl_2): δ 108.3 (d, $^1J_{PRh}$ 205 Hz), −143.0 (sep, $^1J_{PF}$ 711 Hz, PF_6). ^1H NMR (399.8 MHz, $CDCl_3$): δ 7.54 (m, 1H, C_4H_3), 7.42 (m, 2H, Ar), 7.24 (m, 8H, Ar), 6.73 (m, 1H, C_4H_3), 6.42 (m, 1H, C_4H_3), 2.71 (s, 6H, Me). IR (KBr, cm^{-1}): 1570s [ν(C=O)], 837vs [$\nu(PF_6)$].

Synthesis of [Rh(L^2-κ^2*P,O*)$_2$]PF$_6$ 8. NH_4PF_6 (0.255 g, 1.6 mmol) was added to a dichloromethane solution of **L^2** (0.854 g, 3.14 mmol) and [Rh(μ-Cl)(cod)]$_2$ (0.380 g, 0.78 mmol). The mixture was stirred for 3 h, after which the solution was filtered to remove NH_4Cl. The filtrate was evaporated under reduced pressure to give a yellow powder which was recrystallised from dichloromethane–hexane to give **8** as yellow crystals. Yield 1.190 g (96%). Calc. for $C_{28}H_{28}F_6N_6O_2P_3Rh$: C, 42.5; H, 3.60; N, 10.6%. Found: C, 42.5; H, 3.60; N, 10.6%. $^{31}P\{^1H\}$ NMR (161.8 MHz, CD_2Cl_2): δ 104.2 (d, $^1J_{PRh}$ 269 Hz), −143.0 (sep, $^1J_{PF}$ 711 Hz, PF_6). ^1H NMR (399.8 MHz, CD_2Cl_2): δ 7.65 (m, 2H), 6.64 (m, 2H), 6.59 (m, 8H), 6.55 (m, 2H), 6.29 (m, 8H), 2.74 (s, 6H). $^{13}C\{^1H\}$ NMR (C_6D_6, 75.5 MHz): δ 193.7 (s), 133.8 (s), 133.6 (m), 123.7 (m), 116.5 (s), 115.2 (m), 26.9 (s). IR (CH_2Cl_2, cm^{-1}): 1575s [ν(C=O)], 837vs [$\nu(PF_6)$].

Synthesis of [RhCl(L^2-κ^2*P,O*)(L^2-κ^1*P*)] 11. NEt_3BzCl (0.028 g, 0.13 mmol) was added to a dichloromethane solution of **8** (0.100 g, 0.13 mmol). The mixture was stirred for 4 h, filtered then addition of hexane precipitated a red powder which was isolated by filtration, washed with diethyl ether and dried under reduced pressure. Recrystallisation from dichloromethane–hexane gave **11** as red crystals. Yield 0.072 g (84%). Calc. for $C_{28}H_{28}ClN_6O_2P_2Rh$: C, 49.4; H, 4.15; N, 12.3%. Found: C, 49.6; H, 4.22; N, 12.3%. $^{31}P\{^1H\}$ NMR (161.8 MHz, CD_2Cl_2): δ 98.2 (br d, $^1J_{PRh}$ 276 Hz). ^1H NMR (399.8 MHz, CD_2Cl_2): δ 7.23 (br m, 2H), 6.66 (br m, 8H), 6.26 (t, 2H, $^3J_{HH}$ 3.6 Hz), 6.18 (br m, 8H), 5.87 (br m, 2H), 2.49 (br s, 3H). IR (KBr, cm^{-1}): 1632s, 1591s [ν(C=O)]; IR (CH_2Cl_2, cm^{-1}): 1642s, 1592s [ν(C=O)].

Crystallography

Crystallographic data for compounds **2**, **5**·CH_2Cl_2, **6**·C_7H_8, **7b**, **8** and **11** are summarised in Table 8. All data were collected using a Nonius KappaCCD diffractometer with the exception of **5**·CH_2Cl_2 which were collected on an Enraf-Nonius CAD4. Full matrix anisotropic refinement was implemented in the final least-squares cycles for all structures with the specific exceptions described below. All data were corrected for Lorentz and polarisation. Absorption corrections (multiscan) were applied on the basis of their individual merits to data for **2**, **7b** and **8** (maximum, minimum transmission factors were 1.03, 0.91; 1.04, 0.97; and 1.02, 0.98; respectively). Hydrogen atoms were included at calculated positions throughout with the exception of the solvent moiety in **5**·CH_2Cl_2.

The asymmetric unit in **5**·CH_2Cl_2 was seen to consist of one half of a rhodium dimer and one dichloromethane molecule with half site occupancy. The remaining portion of the dimer arises *via* the $1-x, -y, -z$ transformation. Disorder within the sample was evident at the early stages of refinement, whereby the bridging carbonyl and terminal chloride ligands are disordered in a 1 : 1 ratio with a bridging chloride and terminal carbonyl respectively. Moreover, proximity of the solvent molecule in the asymmetric unit to an inversion centre also resulted

Table 8 Crystallographic data for complexes **2**, **5**·CH_2Cl_2, **6**·C_7H_8, **7b**, **8** and **11**

Compound	**2**	**5**·CH_2Cl_2	**6**·C_7H_8	**7b**	**8**	**11**
Empirical formula	$C_{15}H_{14}ClN_3O_2PRh$	$C_{51}H_{42}Cl_4O_4P_4Rh_2$	$C_{41}H_{40}Cl_2N_8O_4P_4Rh_2$	$C_{36}H_{32}F_6N_2O_2P_3Rh$	$C_{28}H_{28}F_6N_6O_2P_3Rh$	$C_{56}H_{56}Cl_2N_{12}O_4P_4Rh_2$
M	437.62	1158.34	1109.41	834.46	790.38	1361.73
T/K	293(2)	293(2)	293(2)	170(2)	170(2)	150(2)
Crystal system	Monoclinic	Monoclinic	Monoclinic	Monoclinic	Monoclinic	Monoclinic
Space group	$C2/c$	$P2_1/n$	$C2/c$	$P2_1/c$	$P2_1/n$	$P2_1/n$
a/Å	23.2510(3)	14.394(2)	19.8250(2)	9.7670(1)	9.0230(1)	18.408(4)
b/Å	8.5470(1)	9.683(2)	11.8230(2)	20.3440(3)	20.4470(2)	9.2298(18)
c/Å	17.3260(2)	17.287(3)	20.9580(3)	17.9680(3)	17.3330(2)	33.971(7)
β/°	105.143(1)	92.93(2)	110.9461(7)	104.8440(9)	101.5720(6)	96.13(3)
U/Å	3323.57(7)	2406.3(7)	4587.74(11)	3451.09(8)	3132.82(6)	5739(2)
Z	8	2	4	4	4	4
D_{calc}/g cm^{-3}	1.749	1.599	1.606	1.606	1.676	1.576
μ/mm^{-1}	1.296	1.081	1.025	0.703	0.773	0.838
Crystal size/mm	0.28 × 0.25 × 0.15	0.20 × 0.20 × 0.15	0.2 × 0.15 × 0.15	0.25 × 0.20 × 0.17	0.25 × 0.18 × 0.10	0.10 × 0.10 × 0.10
Reflections collected	35297	4536	26407	42796	74888	26128
Independent reflections	4856	4227	5218	7921	7159	9154
R(int)	0.0420	0.0167	0.0487	0.0385	0.0391	0.0605
$R1$, $wR2$ [$I > 2\sigma(I)$]	0.0252, 0.0629	0.0475, 0.1166	0.0283, 0.0752	0.0297, 0.1054	0.0322, 0.0867	0.0527, 0.1419
R indices (all data)	0.0302, 0.0651	0.0681, 0.1278	0.0344, 0.0812	0.0351, 0.1116	0.0361, 0.0901	0.0926, 0.1733

in disorder which was successfully modelled. The asymmetric unit in **6**·C_7H_8 was also revealed to be composed of half of one molecule which straddles an inversion centre in addition to half of one toluene molecule proximate to a 2-fold rotation axis. Consequently, the solvent methyl group exhibited disorder, which was readily modelled. In the refinement of **8**, the highest unassigned peaks in the final difference Fourier electron density map were proximate to the hexafluorophosphate anion suggesting some disorder. However attempted modelling of any possible disorder failed to improve the structural refinement. The data for compound **11** are only of moderate quality, as reflected in the larger than desirable error on the unit cell parameter, *c*. These data were collected at a time when our hardware was giving an erroneous 'crash' error when starting some scan sequences. This took considerable time to resolve by which time the sample had degraded, thus the refinement presented is based on 68% of potential unique data.

CCDC reference numbers 184445, 184446 and 211980–211983.

See http://www.rsc.org/suppdata/dt/b3/b306292a/ for crystallographic data in CIF or other electronic format.

Acknowledgements

The authors would like to thank the EPSRC for financial support and Johnson-Matthey plc for a generous loan of platinum metals.

References

1 P. Braunstein and F. Naud, *Angew. Chem., Int. Ed.*, 2001, **40**, 680.
2 C. S. Slone, D. A. Weinberger and C. A. Mirkin, *Prog. Inorg. Chem.*, 1999, **48**, 233.
3 A. Bader and E. Lindner, *Coord. Chem. Rev.*, 1991, **108**, 27.
4 A. D. Burrows, *Sci. Prog.*, 2002, **85**, 199.
5 G. K. Anderson and R. Kumar, *Inorg. Chem.*, 1984, **23**, 4064.
6 E. Lindner, R. Speidel, R. Fawzi and W. Hiller, *Chem. Ber.*, 1990, **123**, 2255.
7 E. Lindner, M. Geprägs, K. Gierling, R. Fawzi and M. Steimann, *Inorg. Chem.*, 1995, **34**, 6106.
8 E. Lindner, K. Gierling, B. Keppeler and H. A. Mayer, *Organometallics*, 1997, **16**, 3531.
9 P. Braunstein, D. Matt, D. Nobel, F. Balegroune, S.-E. Bouaoud, D. Grandjean and J. Fischer, *J. Chem. Soc., Dalton Trans.*, 1988, 353.
10 P. Braunstein, Y. Chauvin, J. Nähring, A. DeCian and J. Fischer, *J. Chem. Soc., Dalton Trans.*, 1995, 863.
11 J. Andrieu, P. Braunstein, F. Naud and R. D. Adams, *J. Organomet. Chem.*, 2000, **601**, 43.
12 C. D. Andrews, A. D. Burrows, J. M. Lynam, M. F. Mahon and M. T. Palmer, *New J. Chem.*, 2001, **25**, 824.
13 C. D. Andrews, A. D. Burrows, J. C. Jeffery, J. M. Lynam and M. F. Mahon, *J. Organomet. Chem.*, 2003, **665**, 15.
14 K. G. Moloy and J. L. Petersen, *J. Am. Chem. Soc.*, 1995, **117**, 7696.
15 R. Jackstell, H. Klein, M. Beller, K.-D. Wiese and D. Röttger, *Eur. J. Org. Chem.*, 2001, 3871.
16 A. D. Burrows, M. F. Mahon, M. T. Palmer and M. Varrone, *Inorg. Chem.*, 2002, **41**, 1695.
17 S. Fischer, L. K. Peterson and J. F. Nixon, *Can. J. Chem.*, 1974, **52**, 3981.
18 A. D. Burrows, M. F. Mahon and M. T. Palmer, *J. Chem. Soc., Dalton Trans.*, 2000, 1669.
19 R. G. Pearson, *Inorg. Chem.*, 1973, **12**, 712.
20 P. Das, M. Sharma, N. Kumari, D. Konwar and D. K. Dutta, *Appl. Organomet. Chem.*, 2002, **16**, 302.
21 I. Le Gall, P. Laurent, E. Soulier, J.-Y. Salaün and H. des Abbayes, *J. Organomet. Chem.*, 1998, **567**, 13.
22 R. W. Reed, B. Santarsiero and R. G. Cavell, *Inorg. Chem.*, 1996, **35**, 4292.
23 A. M. Trzeciak, T. Glowiak, R. Grzybek and J. J. Ziólkowski, *J. Chem. Soc., Dalton Trans.*, 1997, 1831.
24 P. Braunstein, Y. Chauvin, J. Nähring, A. DeCian, J. Fischer, A. Tiripicchio and F. Ugozzoli, *Organometallics*, 1996, **15**, 5551.
25 M. Cowie, *Inorg. Chem.*, 1979, **18**, 286.
26 M. M. Olmstead, C. H. Lindsay, L. S. Benner and A. L. Balch, *J. Organomet. Chem.*, 1979, **179**, 289.
27 G. Liehr, G. Szucsányi and J. Ellermann, *J. Organomet. Chem.*, 1984, **265**, 95.
28 F. H. Allen, *Acta Crystallogr., Sect. B*, 2002, **58**, 380.
29 D. A. Fletcher, R. F. McMeeking and D. Parkin, *J. Chem. Inf. Comput. Sci.*, 1996, **36**, 746.
30 C. Woodcock and R. Eisenberg, *Inorg. Chem.*, 1985, **24**, 1285.
31 D. J. Anderson, K. W. Kramarz and R. Eisenberg, *Inorg. Chem.*, 1996, **35**, 2688.
32 D. J. Irvine, C. Glidewell, D. J. Cole-Hamilton, J. C. Barnes and A. Howie, *J. Chem. Soc., Dalton Trans.*, 1991, 1765.
33 E. Lindner, Q. Wang, H. A. Mayer and A. Bader, *J. Organomet. Chem.*, 1993, **458**, 229.
34 A. D. Burrows, *CrystEngComm*, 2001, **3**, 217.
35 L. H. Pignolet, D. H. Doughty, S. C. Nowicki and A. L. Casalnuovo, *Inorg. Chem.*, 1980, **19**, 2172.
36 I. V. Kourkine, C. S. Slone, C. A. Mirkin, L. M. Liable-Sands and A. L. Rheingold, *Inorg. Chem.*, 1999, **38**, 2758.
37 E. Lindner, Q. Wang, H. A. Mayer, R. Fawzi and M. Steimann, *Organometallics*, 1993, **12**, 1865.
38 P. Braunstein, B. T. Heaton, C. Jacob, L. Manzi and X. Morise, *Dalton Trans.*, 2003, 1396.
39 H. Werner, A. Hampp, K. Peters, E. M. Peters, L. Walz and H. G. von Schnering, *Z. Naturforsch., Teil B*, 1990, **45**, 1548.
40 E. Lindner, Q. Wang, H. A. Mayer, A. Bader, H. Kühbauch and P. Wegner, *Organometallics*, 1993, **12**, 3291.
41 J. A. McCleverty and G. Wilkinson, *Inorg. Synth.*, 1966, **8**, 211.
42 G. Giordano and R. H. Crabtree, *Inorg. Synth.*, 1990, **28**, 88.
43 P. E. Garrou and G. E. Hartwell, *Inorg. Chem.*, 1976, **15**, 646.
44 A. A. Del Paggio, E. L. Muetterties, D. M. Heinekey, V. W. Day and C. S. Day, *Organometallics*, 1986, **5**, 575.
45 J. G. Verkade, *Coord. Chem. Rev.*, 1972/73, **9**, 1.